CHAPTER 3

PARTICLE-IN-CELL (PIC) SIMULATION OF *Ka*-BAND GYRO – TWYSTRON *

*Part of this work has been published as:

Vangalla Veera Babu, M. Thottappan, and Smrity Dwivedi " Design and simulation investigations of a high gain millimeter wave gyro-twystron amplifier," *Journal of Electromagnetic Waves and Applications*, vol. 36, no. 18, pp. 2740-2755, July 2022, doi:10.1080/09205071.2022.2106448.

3.1. Introduction

The electron beam and RF wave interaction mechanism in a gyro-twystron amplifier is quite complex since there are many parameters, factors, and issues that all affect the overall performance of the device at the same time. As a result, in the prior chapter, Chapter 2, nonlinear multimode analyses of a gyro-twystron amplifier were carried out to investigate the device's beam-wave interaction behavior. The nonlinear multimode analysis can exhibit mutual effects among more than one mode, including the operating mode and other competing modes in the interaction structure of the gyro-twystron amplifier. Based on these analyses, computer simulation initiatives have been introduced, and their validity was confirmed by comparing numerical values thus obtained with experimental results. With the advent of powerful computers, simulation and modelling techniques have become widely employed for device design and performance evaluation. These simulation techniques provide useful insight into device behavior while supporting analytical models. The particle-in-cell (PIC) simulation method has been proven useful and practical for investigating gyro-device beam-wave interaction behavior and optimizing their performance.

In the present chapter, the modelling and the electron beam and RF wave interaction behavior study of the gyro-twystron amplifiers is described in detail using a commercially available CST Studio Suite 3D Particle-in-cell (PIC) simulation code. Further, the various sub-assemblies of the gyro-twystron, like gyrating beam source (MIG), beam collector, and RF window, are discussed. Commercially available CST microwave studio is employed to perform the beam absent or cold analysis of each section of gyro-twystron to ensure its frequencies (operating, resonating, and cut off) and operating modes with the desired quality factor. Similarly, the particle in cell (PIC) simulation is performed for the hot analysis or beam present analysis, in which the

interaction of the electron beam and RF wave interaction is studied. The PIC simulation results are validated with the multimode code based on the multimode theory discussed in the chapter 2. Various parameters are varied to optimize the performance of the gyro-twystron amplifier to maximize the performance metrics. The following section discusses the details of electromagnetic simulation approaches and gyro-twystron simulation investigations.

3.2. Design of Electron Beam Source

The performance of any gyro device is highly dependent on the quality of the gyrating electron beam, which is produced by the beam-forming systems, also known as the electron guns. Magnetron Injection Guns (MIGs) have been the typical beam-forming system for gyro devices. The name MIG, as it resembles a magnetron [4], forms a hollow beam of electrons in helical trajectories in the device. MIGs are available in two configurations [125], [126], diode-type MIGs and triode-type MIGs. The diode type MIG has the most basic geometry and structure. It is simple to achieve a durable design with a lower assembly tolerance. The triode-type system has an additional electrode with a potential difference between the cathode and the anode, which needs an additional power source and electric insulation, making it more challenging to fabricate and assemble. It still accomplishes adding another degree of freedom (the voltage on the modulation anode) to further tune the electron beam quality in operation.

In MIG, electrons are emitted from a conical cathode, which is generally temperature limited thermionic cathode, in which current variation is easily possible. The emitted electrons move in the helical path under the influence of the cross-electric and magnetic fields. The efficient operation of the gyro-twystron depends on the quality of the electron beam. Therefore, MIG design parameters, including magnetic

compression ratio, down taper dimension, cathode slant, and cathode anode gap, are optimized according to the requirement of electron beam characteristics in the interaction region [37], [38]. Electron optics (E-GUN) code is now commonly used to explore electron beam propagation without RF conditions. In this section, we designed and optimized a MIG to improve the gyro-twystron amplifier's performance metrics.

3.2.1. Single Anode Magnetron Injection Gun (MIG)

In the current study, a single anode MIG is designed and optimized for *Ka*-band gyro-twystron. The basic parameters of MIG, such as magnetic compression ratio, guiding center radius, cathode radius, beam voltage, cathode slant angle, are calculated using trade-off equations [37, 38]. The electron beam optics E- GUN code [127] is used for electrostatic simulation of MIG, whose geometry and electron beam trajectories are shown in Fig. 6. The optimized design parameters of the single anode MIG are given in Table 3. 1.

Table 3. 1 Design Parameters of Diode MIG

Parameters	**Values**
Beam voltage	65kV
Beam current	10A
Guiding center radius	2.64 mm
Axial velocity spread	3.72%
Transverse velocity spread	1.43%
Velocity ratio	1.4
Cathode current density	3.45 A/cm^2
Magnetic compression ratio	16.6

The parametric study of the MIG is carried out by varying beam voltage and cathode magnetic field. Fig. 7 (a) depicts that when beam voltage is 65 kV, the velocity spread is

~4 %, and velocity ratio is 1.4. The value of velocity ratio (α) decreases linearly with the cathode magnetic fields from 0.076 T to 0.084 T. The value of velocity spread also decreases with an increase in cathode magnetic field [Fig. 7 (b)].

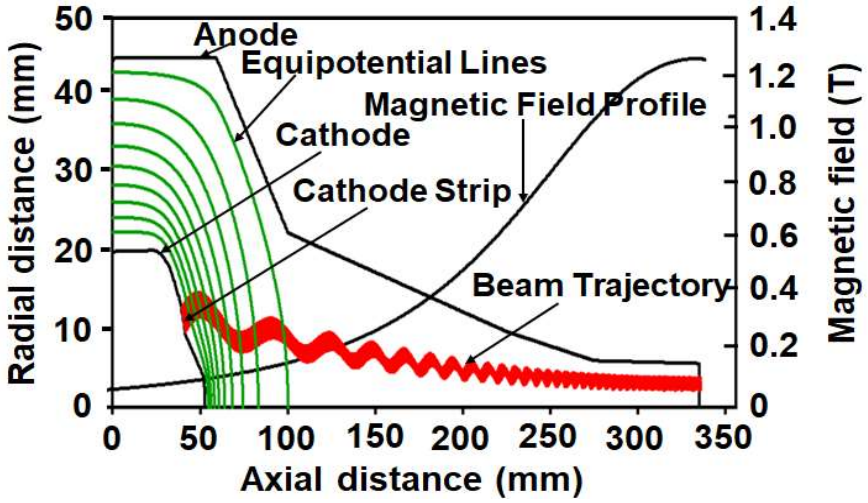

Fig. 3. 1. Electron beam trajectories, magnetic field profile, and equipotential lines of diode type MIG for *Ka*-band gyro-twystron.

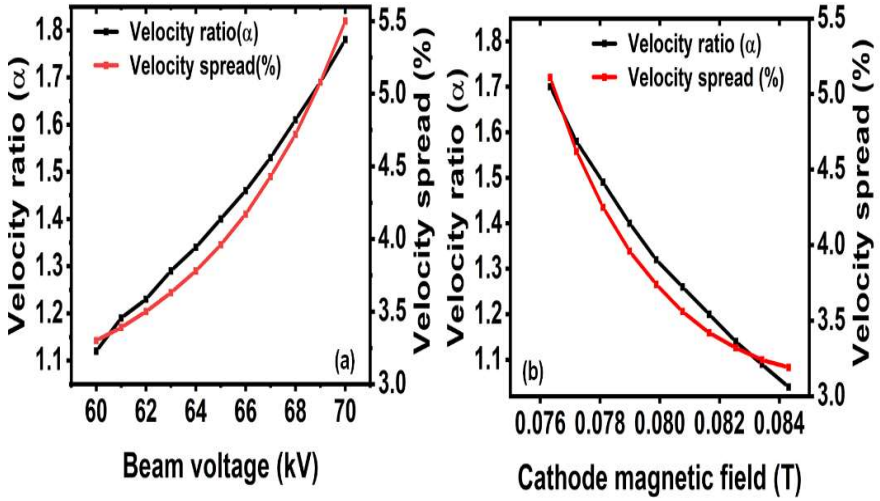

Fig. 3. 2. Velocity ratio and velocity spread variation for **(a)** beam voltages **(b)** cathode magnetic field.

3.3. PIC Simulation Study of Single Cavity *Ka*-Band Gyro-twystron

Today, microwave engineers depend extensively on flexible simulation tools for designing and developing VEDs due to manufacturing challenges and application-specific design, which raises the cost of VED development. Before making significant

efforts in experimental development and testing, virtual testing of VEDs is required to forecast design and operating parameters. The theoretical study's acceptable anticipated parameters allow for device fabrication and development [67], [128]. Commercially available, 3D simulation tools reduce device development time and costs and allow users to virtually observe electron beam generation and beam wave interactions in the interaction region and provide an option to optimize the design before the device is physically constructed. Due to the above benefits, simulation tools should be used as part of high-power gyrotron device design and development.

There are several 3D simulation tools, such as CST, HFSS, COMSOL, and XFdtd, etc., in which the real performance of the amplifier could be realized under experimental conditions, i.e., in the presence of an electron beam (under hot conditions). These tools working on based on different numerical techniques, such as CST is based on the Finite Integration Technique (FIT), HFSS, and COMSOL, which is based on the Finite element method (FEM), XFdtd, is based on the Finite-Difference Time-Domain method (FDTD), etc. The commercially available CST studio suit simulation tool is used to validate the nonlinear multimode analytical finding of the current single cavity *Ka*-band gyro-twystron. The 3-D simulation tool provides the user with a virtual environment to monitor the propagation of RF waves, the gyrating beam, and the interaction of beam waves. The simulation tool can be used to study the device's operational limits and the detrimental effect on device functioning caused by changes in expected parameters.

3.3.1. Particle-In-Cell (PIC) Simulation

CST Particle Studio" is a specialized module for the fast and precise study of charged particle dynamics in 3D electromagnetic fields and the simulation of electromagnetic field-charged particle interactions. Incorporating particles into these

numerical field calculating approaches necessitates particle-in-cell procedures in which particles with similar physical charge and specific mass ratio are represented as units. This approach to macro particle representation incorporates millions of unit particles to produce an electron beam. The core of PIC simulation is the computation of Maxwell equations and Lorentz force equations

CST Microwave Studio provides users with six field solvers, electrostatic, magneto static, Eigen mode solver, particle tracking solver, particle in cell solver (PIC), and wakefield solver for a wide range of electromagnetic problems in various structures. In the present simulations study, we use Eigen mode particle in cell solver (PIC) solvers for beam absent and beam present analysis. The Eigen mode solver is used to simulate closed resonant structures. The Eigen mode solver is highly efficient in circumstances of loss-free substantially resonant structures where the fields (the modes) must be determined. [CST user's handbook (2022)] The Eigen mode solver cannot be used with open borders or discrete ports. Tetrahedral or hexahedral meshing is employed in the Eigen mode solver, which is compatible with CST Particle Studio and Mphysics Studio. CST MWS is recommended over other simulation tools for cold simulation studies because of its comprehensive and flexible approach to problem-solving. To investigate the electron beam dynamics, the particle source solver is used. The PIC solver simulates the evolution of charged particles in self-consistent electromagnetic fields. Moreover, the static or analytic field distributions can easily be added to the PIC simulation. The feature of the PIC solver includes the charged particles emission from arbitrary surfaces or single points. The PIC solver is used to compute RF wave, electron beam propagation, and beam-wave interaction using Maxwell and Lorentz force equations. CST particle studio is based on the FIT method, which uses perfect boundary

approximation. Unlike MAGIC-3D, the CST Particle studio PIC solution provides multimode computing capabilities, particle tracking, and Wakefield solvers.

CST Particle Studio involves four major steps before proceeding with the solution of beam-wave interaction problems. Before examining beam wave interactions with PIC simulation, a 2D cross-sectional view of the RF interaction structure must be defined for which simulation is required. In the absence of a beam, the cavity is simulated using the CST microwave studio's Eigen mode solver. For the absent beam case, the cavity is simulated using the Eigen mode solver of the CST microwave studio. After defining the shape, the simulation frequency range should be defined based on the cavity's operating region. The main steps of performing the simulation can be found in the 'quick start guide' feature of the software code, the corresponding applicable solver module. A waveguide port is defined at the output section to identify the signal amplitude corresponding to the various modes. In order to make the beam wave interaction in the interaction region, the desired cross-section of an electron beam with the necessary beam parameters is injected into the electromagnetic structure using the DC emission model. The external magnetic field must be applied to focus the electron beam inside the interaction structure in a well-defined trajectory. Understanding the behavior of an electromagnetic device necessitates knowledge of the electromagnetic field distribution. Thus, essential frequency points are defined at which the solver will record the fields established, and these field samplers are referred to as Field Monitors. These are primarily of two types: electric field (*E*-Field) monitors and magnetic field (*H*-Field) monitors, with the former investigating electric field distribution and the latter investigating magnetic field distribution. The specified dialogue box defines the monitoring of the electric and magnetic fields and the power inside the cavity. Particles are also monitored in 2D or 3D planes to provide information regarding particle

disturbance in terms of energy or phase and bunching phenomena. The phase space monitors are defined for this purpose. The particles are monitored for their momentum, position, and so on at a set of time intervals, i.e., over the complete or partial duration of simulation, to gain the modulation of energy or momentum among particles.

3.3.2. CST Modelling

The modelling of the RF interaction structure of the *Ka*-band gyro-twystron is implemented using CST Studio Suite [Fig. 3.3], and the same is validated with the help of nonlinear multimode analysis described in Chapter 2. CST Microwave studio PIC solver is selected to study the RF propagation characteristics through the techniques discussed in the previous section. A gyro-twystron amplifier's PIC simulation comprises mainly three steps. Initially, the RF interaction structure of a gyro-twystron amplifier is modelled utilizing the pertinent design parameters for modelling. Secondly, the desired mode of operation at the required frequency is chosen by modelling the structure without a beam (cold analysis) with an Eigen mode solver. The device's performance in terms of RF output power and gain is determined by modelling the structure in the presence of a beam (hot analysis). In order to study the multimode interaction behavior of the device, the signal amplitudes corresponding to all possible modes in the output waveguide are generated. Each RF sub-section is modelled independently with structural design specifications, as given in Table 3. 2.

The input cavity and output waveguide are intended to operate in a low-loss azimuthally symmetric TE_{01} mode with the highest electric field at their center. The input Cavity and drift tube are modelled using an annealed copper with a conductivity

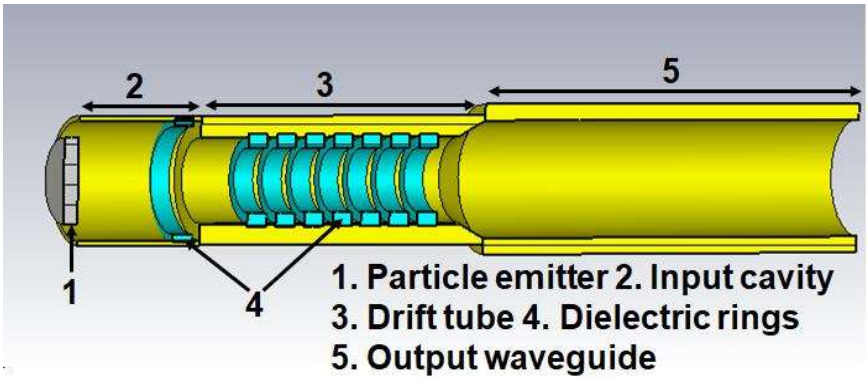

Fig. 3. 3. CST 3-D simulation model of the single cavity *Ka*-band gyro-twystron.

Table 3. 2 Design Parameters of *Ka*-Band Gyro-twystron

Parameters	**Values**
Operating Frequency (GHz)	35
Operating mode	TE_{01}
Beam current (A)	10
Beam voltage (kV)	65
Velocity ratio	1.4
Cavity length (mm)	12.8
Cavity radius (mm)	5.55
Magnetic field (T)	1.31
Drift tube length (mm)	30
Drift tube radius (mm)	4
Output Waveguide length (mm)	40
Output Waveguide radius (mm)	5.5

of 5.8×10^7 S/m. Aluminium nitride-silicon carbide (AlN-SiC) with a dielectric constant of 11-2.2j and a loss tangent of 0.2 at 35GHz is shown in Fig. 3. 4. It is loaded in the input cavity end to eliminate oscillations and achieve the necessary quality factor. A field-free drift region is positioned between the cavity and the waveguide to provide isolation between different components of the RF circuit. To model the field-free drift

section, the radius of the drift section is fixed such that the operating frequency is well above the drift tube's cut-off frequency for an operational mode. It is filled with lossy ceramic rings of Aluminium nitride-silicon carbide (AlN-SiC) with a length of 30 mm and a radial thickness of 4 mm to absorb the electromagnetic (EM) fields that leak into the drift section. To overcome abrupt reflections, a nonlinear section is present between the drift section and the output waveguide. The outside radius of the waveguide is chosen so that the waveguide's cut-off frequency is just below the operating frequency. To achieve stability against competing modes. Using the inbuilt meshing approach in The CST Studio suite, the entire modelled structure is divided into small, individually split cells.

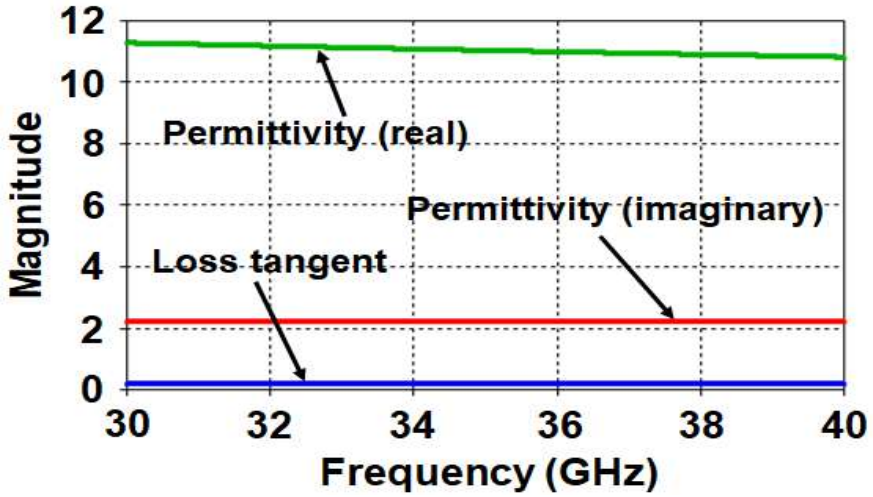

Fig. 3. 4. Dielectric properties of AIN-SiC in Ka-band.

The hexahedral meshing approach is employed in the current design to transform the design structure into tiny cells. The entire simulation structure has meshed with ten cells per wavelength and a mesh limit of twenty. Constraints such as operating wavelength, simulation time, memory size, and so on determine the maximum number of meshes. Furthermore, the boundary condition was implemented in such a way that the tangential component of the electric field vanished (E_t= 0) at the outer walls of the RF circuit,

which has the shape of a rectangular bounding box because it follows the Cartesian system and the background material is a vacuum.

3.3.3. Beam absent Study

In order to examine the electromagnetic characteristics of the gyro-twystron input cavity, Eigen mode analysis is performed in the absence of an electron beam before PIC simulation to ensure the operating mode, frequency and to compute the appropriate Q-factor. The electric field pattern is observed to confirm the presence of a particular mode inside the cavities. The present input cavity of gyro-twystron operating in TE_{01} is realized by observing the electric field between the wall and the center of the RF structure, shown in Fig.3.5.

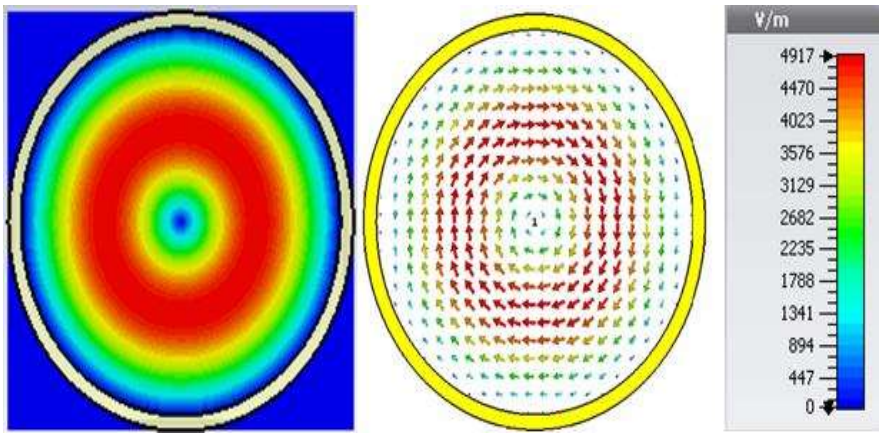

Fig. 3. 5. (a) Contour plot and **(b)** vector plot of the TE_{01} mode in cavity.

Further, to obtain the desired quality factor of the input cavity, i.e., ~200, the cavity end is loaded with aluminium nitride-silicon carbide (AlN-SiC) having a dielectric constant of 11- 2.2*j* at 35GHz. The input cavity resonant frequency is verified through the post-processing of the transient solver of CST MWS is sown in Fig. 3. 6

Since the drift tube is modeled to provide the isolation between the cavity and waveguide, it also provides the cutoff to the operating TE_{01} mode. Its radius is calculated such that to satisfy the condition for the drift radius $rb < rd < rc$ to avoid the

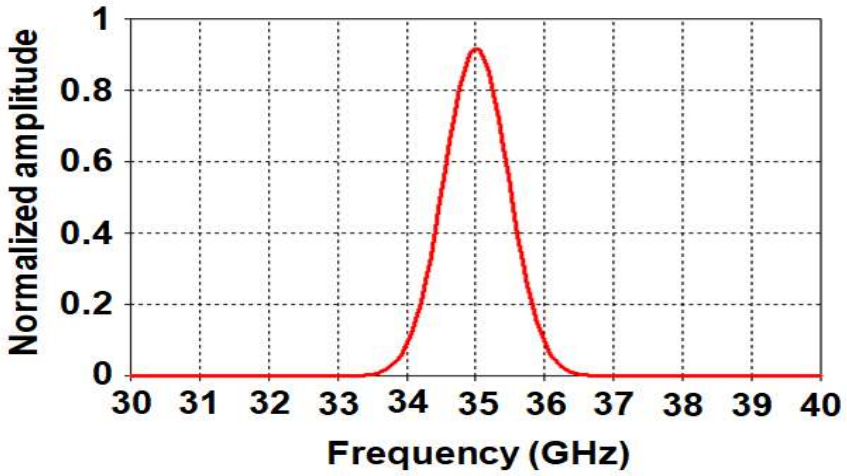

Fig. 3. 6. The resonating frequency of the cavity.

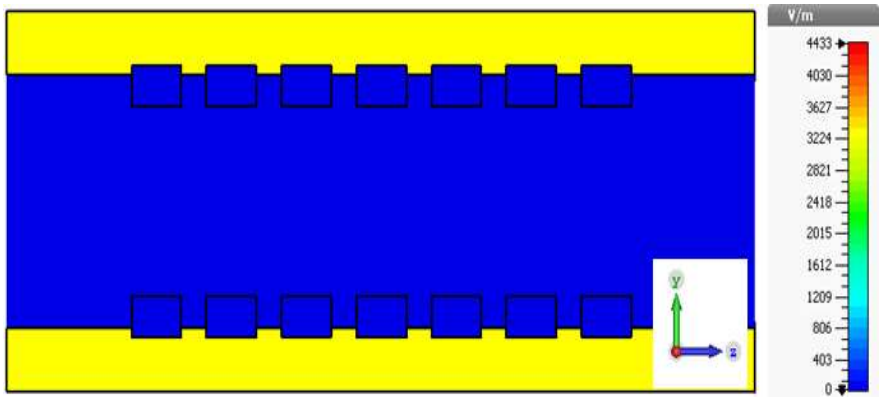

Fig. 3. 7. Electric field distribution in the drift tube.

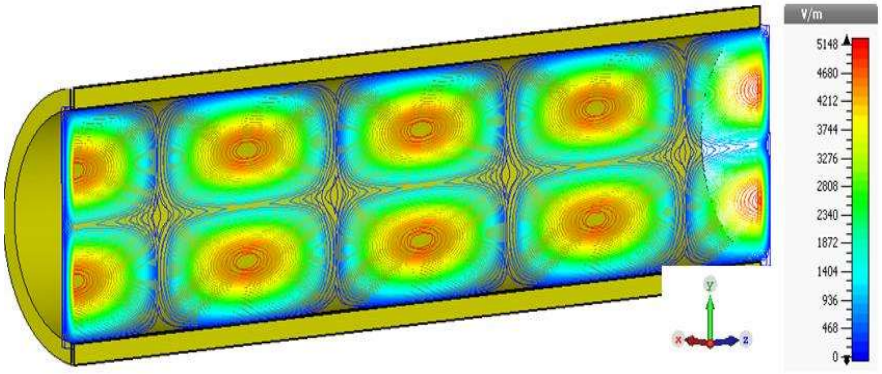

Fig. 3. 8. Field distribution in the output waveguide.

field propagation, where *rb* is electron beam guiding radius, *rd* is drift tube radius, and *rc* is cavity radius. The drift tube length (*Ld*) is chosen by the cold cavity dispersion relation [29] is discussed in chapter 2. The drift tube is loaded with AlN-SiC dielectric rings to attenuate the TE_{21} and TE_{11} modes and to absorb any field leakage between adjacent sections. In the present design, the drift tube's radius and length are calculated as~4 mm and ~ 30 mm, respectively, to have the isolation of ~50 dB between the input cavity and output waveguide. Figure 3.7 shows that the electric field confinement is lowest in the drift tube region, confirming that the RF wave is substantially suppressed in the drift tube. The output waveguide radius is fixed by the cutoff frequency, which is below the operating frequency of the amplifier. The transient analysis of the traveling wave section yields a cutoff frequency of 33 GHz for the TE_{01} mode. The propagation of the TE_{01} mode in the output traveling wave section is confirmed by the electric field confinement [Figure 3.8].

3.3.4. Beam Wave Interaction Study

After the simulation of the beam-absent condition has been performed, the simulation proceeds for the beam-present condition. Further, 3D Particle-In-Cell (PIC) simulation is carried out to determine the gyro-twystron characteristics like output RF power, bandwidth, gain, and efficiency in the presence of an electron beam. The interaction strength between the electron beam and RF wave depends on the gyrating electron beam quality. Through the DC emission model, the particle source (i.e., cathode) emits the gyrating electron beams in the PIC solver of the CST particle studio. The cathode is created by feeding structural parameters and beam parameters via specified emission models. The cathode is made using a circular particle source with several emission models. The emitting face is defined by a PEC or non-PEC surface. The DC emission model is chosen from among the four emission models to define the

kinetic characteristics of the electron beam. The voltage term in the DC emission model is defined in terms of many kinetic factors, including energy, momentum, Lorentz factor, and velocity. The current term in the model is specified directly. The DC emission model's oblique emission setting defines the beam velocity ratio, also known as the pitch factor, as the inverse of the tangent angle term and inserts it into the term of angle theta. At the same time, the kinetic setting of the DC emission model is directly fed the spread in beam velocity. In a circular particle source, the outer and inner radii are equal to the sum and difference of the guiding center radius and the Larmor radius, respectively. In the current simulation, the beam voltage of 65 kV is converted into velocity as a kinetic type, and a pitch factor of 1.4 is converted to an angle of 54.50 degrees. The outer radius and inner radius of the gyrating beams are imported from the EGUN modelling and simulation, as indicated in Table 3. 1, and fed into the emitter circle of the DC emission model in order to avoid collisions with the structure wall.

3.3.5. Results and Validation

In the present simulation, the angular electron beam with current of 10A, voltage of 65 kV with a 1.4 velocity ratio under the magnetic field 1.31 T, which enters the input cavity, where electrons motion is perturbed due to the RF input, electrons getting modulated, and these modulated electrons form a bunch in the drift region. The bunched electrons move towards the non-resonant waveguide, interact with the EM wave, and transfer their kinetic energy to the wave resulting in the RF signal amplification. The RF output signal electric field amplitude of operating mode (TE_{01}) and other competing modes, including TE_{11}, TE_{21}, and TE_{02}, are shown in Fig. 3. 9. The temporal growth of electric field amplitudes of the competing modes are much smaller than the desired TE_{01} mode. Fig. 3.10 (a) shows the instantaneous power of 480kW or averaged over an RF period of actual power 240kW, generated in the preferred operating mode, calculated by

E-field amplitude as shown in Fig. 3.9. The developed output RF signal frequency spectrum shown in Fig. 3.10 (b) confirms the device operate, at the targeted frequency i.e. 35GHz. The PIC simulation results are validated with nonlinear multimode analysis discussed in the preceding section. The nonlinear multimode analysis shows ~237kW of power in TE_{01} mode and much less power in other competing modes.

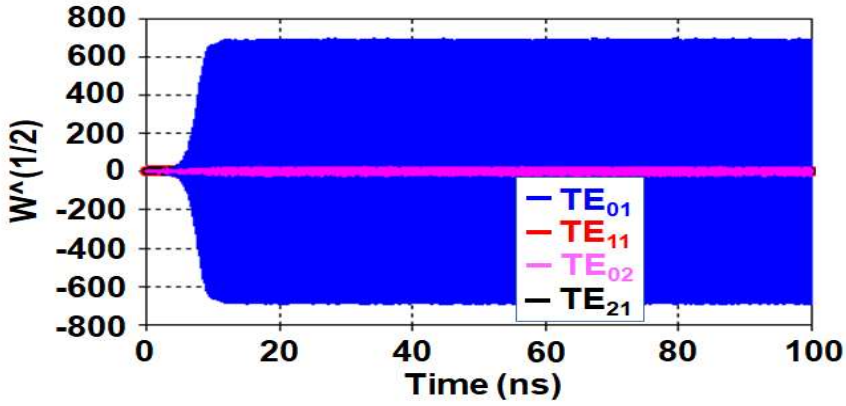

Fig. 3. 9. The amplified output signal electric field strength in operating TE_{01} mode and other competing TE_{11}, TE_{21}, TE_{02} modes.

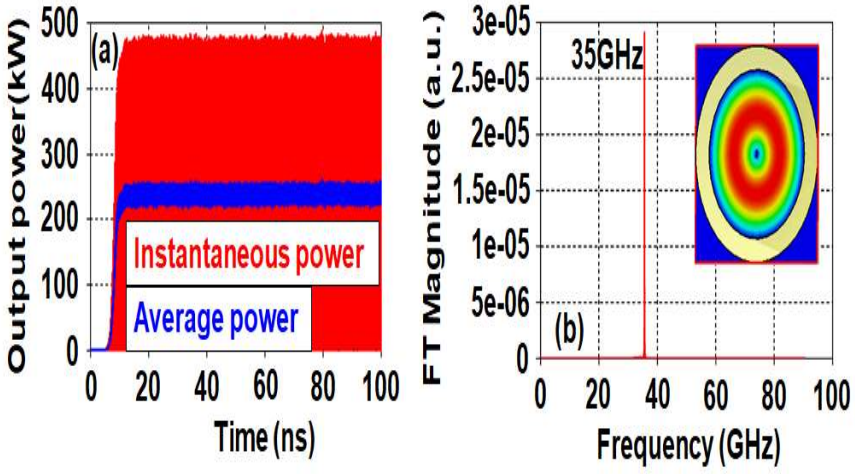

Fig. 3. 10. (a) output power signal grown in TE_{01} mode **(b)** FT signal with contour plot (inset).

The power in desired TE_{01} mode calculated using multimode analysis and PIC simulation is in good concurrence. The output power and bandwidth of the current

amplifier have been calculated at different velocity spreads. In the PIC simulation, the kinetic spread with uniform distribution is set to estimate the effect of beam velocity spreads on gyro-twystron characteristics. The RF output power and 3 dB bandwidth of ~240kW and ~2GHz are achieved for zero velocity spread. It is observed that the amplifier output power decreases as the velocity spread increases. The output power and 3-dB bandwidths were reduced to 205kW and ~1.45GHz for a 4% velocity spread, as shown in Fig. 3. 11.

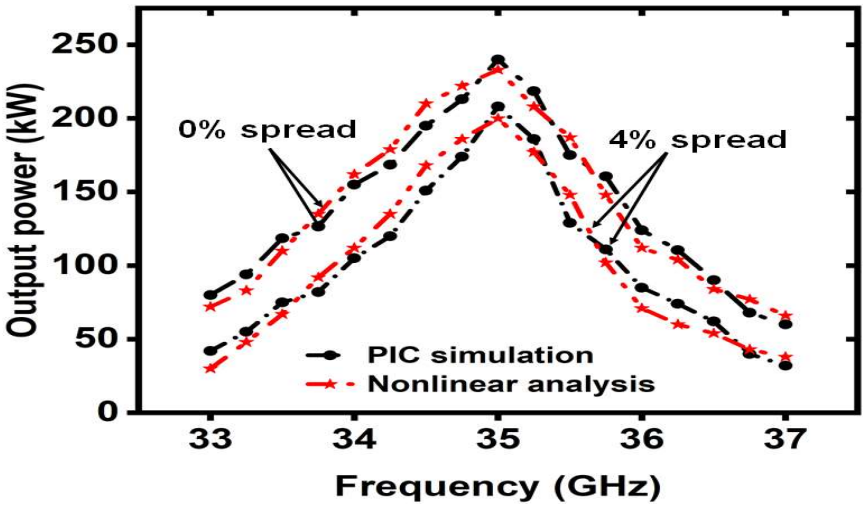

Fig. 3. 11. Comparison of output power between PIC simulation and analytical methods.

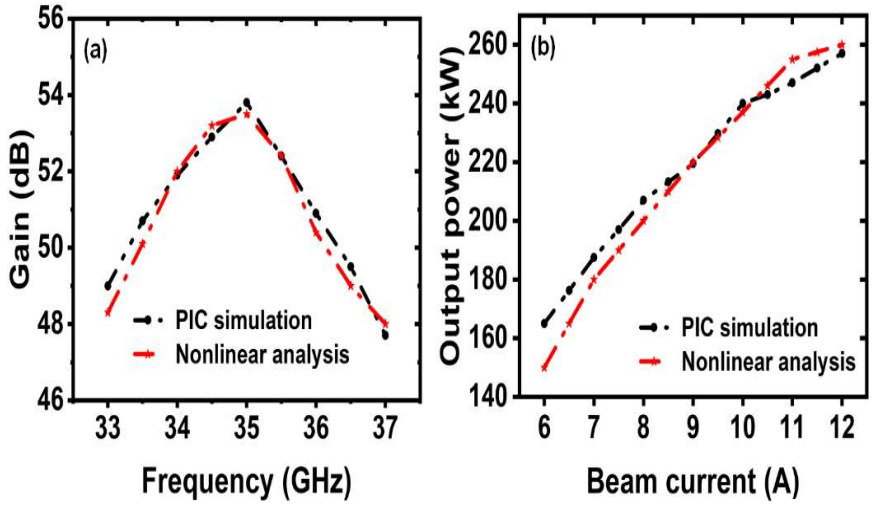

Fig. 3. 12. Comparison of PIC simulation and nonlinear analysis **(a)** Gain versus frequency at 1 W input power **(b)** output power versus beam current at 35 GHz and at 1 W input power.

Furthermore, the performance of the present single cavity gyro-twystron is studied by calculating the saturated RF power and gain through non-linear theory and PIC simulation [Fig. 3. 12(a)].The dependency of RF output power on the beam current [Fig. 3. 12(b)] shows that the maximum output power and efficiency are achieved for 65kV, 10 A electron beam.

3.4. Design of the Output System

3.4.1. Undepressed Collector

After the beam wave interaction, the next goal is to collect the spent electron beam by means of collector as well to collect the generated RF wave for transmission via RF output window. Collector is a simple cylindrical waveguide, and the required magnetic field in this section to intercepts electrons on a collector wall was calculated by using the adiabatic condition [129]

$$B_c(z) = B_0\left[r_{g0} + r_{l0}\sin\phi(z)/R_c\right] \tag{12}$$

where B_0, r_{l0}, r_{g0} magnetic field, Larmor radius, and guiding beam radius in the interaction circuit. $\phi(z)$ is electron angular phase, and R_c is the collector radius. The collector is designed using the E-GUN code, in which 30 beamlets with electron beam energy distribution are considered. These beamlets represent the initial power of the electron beam, which is equivalent to 650 kW, after the beam wave interaction, the RF power of 240 kW is extracted. The remaining power of the electron beam of 410 kW is dissipated on the collector wall surface. The average spent electron beam power with a 10% duty cycle is 41.0 kW. The electron beam is distributed over 280 mm. Fig. 3. 13 illustrates the geometry and trajectories of the spent electron beam. The maximum load on the wall at the collector surface is 0.116 kW/ cm^2, which is below the 1kW/ cm^2 limit.

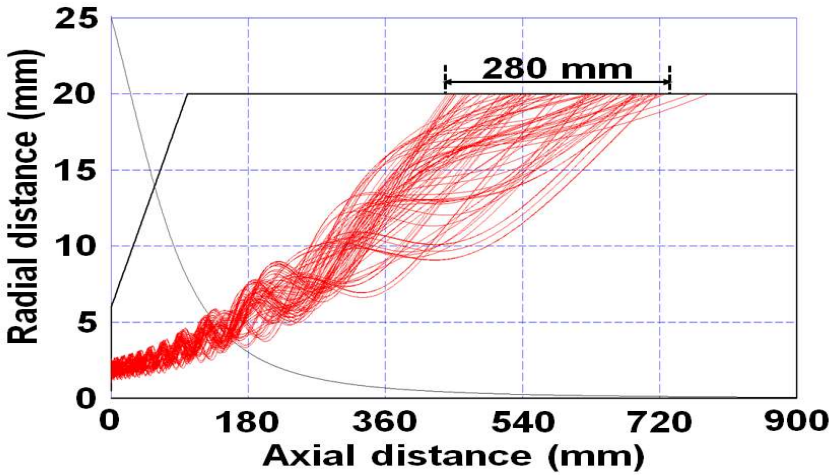

Fig. 3. 13. Geometry and Electron beam trajectory of the undepressed collector.

3.4.2. Design of Single Disc RF Output Window

The RF output window is used in the output section to take out the power from the vacuum to the atmosphere with the minimum reflections for the desired operating mode [5]. The single disc type RF window analysed based on the scattering matrix formulation and modelled [5, 130] in CST microwave studio is shown in Fig. 3. 14. The disc thickness D is given by

$$D = n\lambda \Big/ 2\left(\varepsilon_r\right)^{1/2} \tag{13}$$

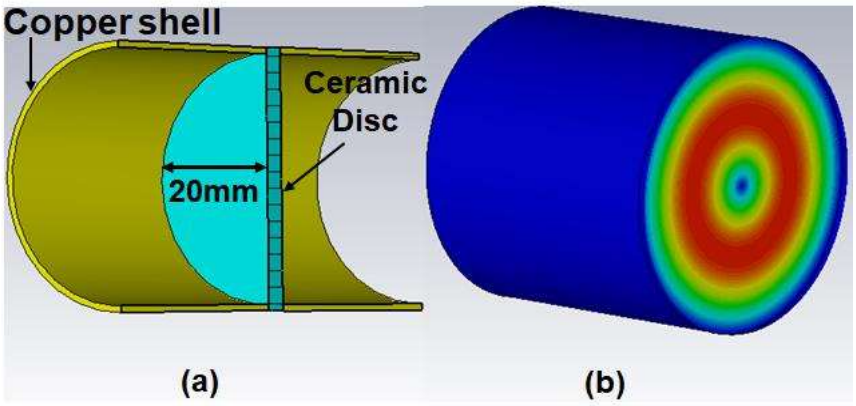

Fig. 3. 14. **(a)** Cross-section view of the single-disc window and **(b)** contour plot of TE_{01} mode E-field inside the single-disc RF window.

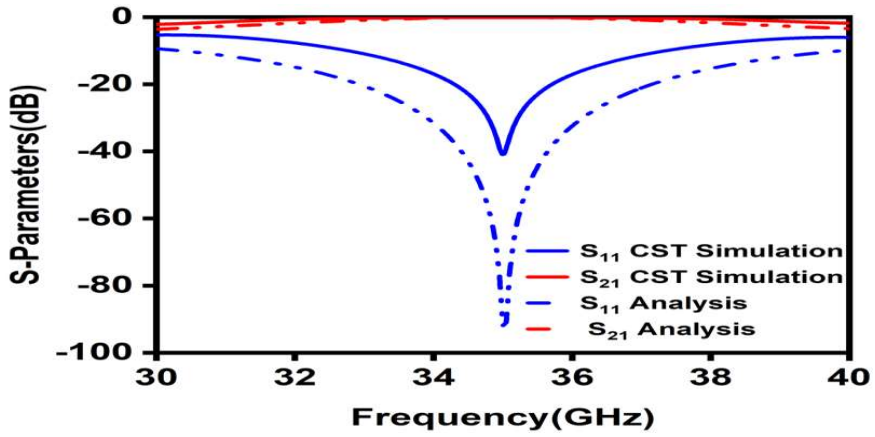

Fig. 3. 15. Comparison of analytical and simulation of reflection (S_{11}) and transmission (S_{21}) coefficient for TE_{01} mode of single disc RF window.

where ε_r represents the dielectric constant of the material, n is an integer. The boron nitride material has been used in the output window, with a disc thickness and radius of 3.9, 20 mm, the dielectric constant of 4.7, and the loss tangent is 0.00115 at 35GHz. Fig. 3. 15 shows the comparison of analytical and simulation (CST MWS) of the transmission coefficient (S_{21}) and reflection coefficient (S_{11}) at 35GHz, respectively.

3.5. Conclusion

A single cavity *Ka*-band gyro-twystron has been modeled and studied for its beam-wave interaction behavior using a commercially available 3D electromagnetic simulation tool, "CST Particle Studio". The design is started with the modelling of single anode MIG that able to generate a good quality gyrating electron beam having a 4% velocity spread and 1.4 velocity ratio followed by the design of RF interaction circuit. The present design of gyro-twystron has been validated with the proposed analytical model of gyro-twystron is discussed in chapter 2. In the PIC simulation, cold analysis (beam absent) and hot analysis (beam present) of different sections of the gyro-twystron structure have been demonstrated. Cold simulation has been performed using an eigenmode solver to examine the cavity specific mode and frequency of operation.

The presented simulations of the amplifier have predicted an RF output power of ~240 kW at 35 GHz with ~37 % efficiency, ~53 dB gain, and a 3-dB bandwidth of ~2 GHz. As an output section, a collector was designed to collect the spent electrons with a wall loading of 0.116 kW /cm^2, and also a single-disc RF window was designed and studied for its good propagation characteristics for the collection of generated RF power. The current gyro-twystron performance metrics have been observed and it has found that the present hybrid amplifier is a viable competitor to the existing *Ka*-band millimeter wave gyro-amplifiers.